

New Algorithm for Level Set Evolution without Re-initialization and Its Application to Variational Image Segmentation

Cunliang Liu

College of Information Engineering, Qingdao University, Qingdao, China
Email: liucl@qdu.edu.cn

Zhenkuan Pan, and Jinming Duan

College of Information Engineering, Qingdao University, Qingdao, China
Email: zkpan@qdu.edu.cn, duanmujinming@126.com

Abstract—Traditionally variational level set model for image segmentation is solved by using gradient descent method, which has low computational efficiency and needs complex re-initialization of level set functions as signed distance functions. In this paper, we first reformulate the variational model as a constrained optimization problem. Then we present an augmented Lagrangian projection method to preserve signed distance functions and accelerate the implementation. By introducing auxiliary variables, we convert derivative constraints to algebraic equations with simple projection. We apply the proposed algorithm to the two-phase/multiphase Chan-Vese models. Numerical results are provided to compare our algorithm with some others, which demonstrate effectiveness and efficiency of our approach.

Index Terms—level set method, signed distance function, augmented Lagrangian method, projection, segmentation

I. INTRODUCTION

In the last twenty years, many of the most general segmentation models have been solved by the level set method (LSM) [1-3]. The basic idea of the LSM is to implicitly represent a contour or interface as the zero level set of a higher dimensional function, called a level set function (LSF), and formulate the motion of the contour as the evolution of the LSF. For closed contours, signed distance functions (SDFs) were originally adopted to represent LSFs. Some recent developments have proposed to use label functions [4], rather than SDFs, to represent contours. This change allows us to use convex relaxation techniques [5] and fast algorithms [6-8] to provide effective alternatives to distance preserving LSMs. Nevertheless, the LSM for image segmentation uses zero level set of a continuous SDF to express contour, and the geometric features such as normal, curvature can be calculated naturally, which is very convenient to post processing of curves and surfaces [9]. For this reason, it is important to design fast and accurate algorithms for distance preserving level set methods.

In conventional level set formulations, the LSF is no longer preserved as an SDF during contour evolution. To overcome this difficulty, two approaches have been suggested to restore the regularity of the LSF and maintain stable interface evolution. Re-initialization [10] is the most common method, which is performed by periodically stopping the evolution and reshaping the degraded LSF as an SDF. However, this approach introduces the questions of when and how to re-initialize the LSF. Also, it may incorrectly move the zero level set away from the expected position. In order to avoid re-initialization, the second method aims at constraining the LSF to preserve an SDF during the contour evolution [9, 11-15]. In [11], the authors introduce a new formulation to restrict the LSF to an SDF. But this formulation consists of three PDEs, which makes the numerical implementation more difficult than the standard LSM. More recently, Li et al. [12] has proposed to add a penalty term into the original energy functional. The penalty term eliminates the need for re-initialization. However, the time step of their method is restricted by the Courant-Friedrichs-Lewy (CFL) condition [16] and the SDF property is only encouraged but not enforced. In [14], Liu et al. proposes an augmented Lagrangian method (ALM) to get rid of re-initialization. Their method simplifies the treatment of constraint greatly, but it does not avoid the computation of curvature, which is time-consuming.

In this paper, we propose a constrained optimization approach, split augmented Lagrangian projection method (SALPM), to get rid of re-initialization and improve the computation efficiency. We incorporate the variable splitting technique to update the Lagrange multiplier, and constrain level set functions to stay distance functions via direct projection. We apply our algorithm to the Chan-Vese models [17, 18]. Comparisons with other methods have shown the high efficiency of our proposed approach.

The rest of this paper is organized as follows. In Section II, we review briefly the LSM applied to image segmentation. In Section III, we discuss the framework of our new model in detail. Numerical results are given in Section IV. Section V draws the conclusions.

Corresponding author: Cunliang Liu

II. RELATED WORKS

A. LSM and VLMS

We first recall the traditional LSM. Let $\Omega \subset R^2$ be an open bounded domain, $f(\mathbf{x}) : \Omega \rightarrow R$ be a given image, where $\mathbf{x} = (x, y)$ is a pixel in Ω . The LSF ϕ is normally defined as an SDF

$$\phi(\mathbf{x}, t) = \begin{cases} d(C(t), \mathbf{x}) & \mathbf{x} \in \text{inside } C(t) \\ 0 & \mathbf{x} \in C(t) \\ -d(C(t), \mathbf{x}) & \mathbf{x} \in \text{outside } C(t) \end{cases} \quad (1)$$

where $d(C, \mathbf{x})$ denotes the Euclidean distance from \mathbf{x} to C . A constraint to (1) is the equation

$$|\nabla \phi(\mathbf{x}, t)| = 1 \quad (2)$$

To satisfy (2), [10] used a re-initialization scheme to solve the following equation to steady state

$$\begin{cases} \phi_t + \text{sign}(\phi_0)(|\nabla \phi| - 1) = 0 & \text{in } \Omega \times R \\ \phi(\mathbf{x}, 0) = \phi_0 & \text{in } \Omega \end{cases} \quad (3)$$

where ϕ_0 is the function to be re-initialized.

The variational LSM (VLMS) proposed in [19] offers us a way to embed the LSF directly into the energy functional by utilizing the following facts

$$|C| = \int_{\Omega} \delta(\phi) |\nabla \phi| dx, \quad |S| = \int_{\Omega} H(\phi) dx \quad (4)$$

In the above, $|C|$ is the length of C , $|S|$ is the area of S (an open set $S \in \Omega$, i.e. $C = \partial S$). $H(z)$ and $\delta(z)$ are, respectively, Heaviside function and Dirac delta function. To avoid singularity in numerical implementation, $H(z)$ and $\delta(z)$ are usually expressed in regularized versions with parameter $\varepsilon > 0$ to approximate the original ones as

$$H_{\varepsilon}(z) = \frac{1}{2} + \frac{1}{\pi} \arctan\left(\frac{z}{\varepsilon}\right), \quad \delta_{\varepsilon}(z) = \frac{1}{\pi} \frac{\varepsilon}{z^2 + \varepsilon^2} \quad (5)$$

B. The Chan-Vese Model without Re-initialization

We here adopt the Chan-Vese model for image segmentation, as it represents a large class of active contour models published in the literature. The Chan-Vese model proposed to use m level set functions to represent $n = 2^m$ phases. If $m = 1$, it is called the two-phase Chan-Vese mode, otherwise it is the multiphase Chan-Vese model [17, 18].

For $i = 1, 2, \dots, n$ and $j = 1, 2, \dots, m$, let $(b_{i-1}^1 b_{i-1}^2 \dots b_{i-1}^m)$ be the binary representation of $i-1$, where $b_{i-1}^j = 0 \vee 1$. The characteristic function $\chi_i(\mathbf{x})$ can be written as the following general expression [20]

$$\chi_i(\mathbf{x}) = \prod_{j=1}^m \left(b_{i-1}^j + (-1)^{b_{i-1}^j} H_{\varepsilon}(\phi_j) \right) \quad (6)$$

where ϕ_j is the level set function. The Chan-Vese model becomes the following minimization problem

$$\min_{\phi_j, u_i} \left\{ \sum_{j=1}^m \gamma \int_{\Omega} \delta_{\varepsilon}(\phi_j) |\nabla \phi_j| dx + \sum_{i=1}^n \int_{\Omega} Q_i(u_i, \mathbf{x}) \chi_i dx \right\} \quad (7)$$

where γ is a positive tuning parameter, u_i is the mean intensity value, and $Q_i(u_i, \mathbf{x})$ is defined as $(u_i - f)^2$.

Considering the constraint (2), we can formulate the problem (7) as a constrained minimization problem

$$\min_{\phi_j, u_i} \left\{ \sum_{j=1}^m \gamma \int_{\Omega} \delta_{\varepsilon}(\phi_j) |\nabla \phi_j| dx + \sum_{i=1}^n \int_{\Omega} Q_i \chi_i dx \right\} \text{ s.t. } |\nabla \phi_j| = 1 \quad (8)$$

In order to force the LSF to be an SDF during evolution, great efforts have been made to enforce (1) to satisfy (2). The authors in [12] add a quadratic penalization term of (2) into the functional and obtain the following unconstrained minimization problem

$$\begin{aligned} \min_{\phi_j, u_i} \left\{ \sum_{j=1}^m \gamma \int_{\Omega} \delta_{\varepsilon}(\phi_j) |\nabla \phi_j| dx + \sum_{i=1}^n \int_{\Omega} Q_i \chi_i dx \right. \\ \left. + \sum_{j=1}^m \frac{\mu}{2} \int_{\Omega} (|\nabla \phi_j| - 1)^2 dx \right\} \end{aligned} \quad (9)$$

The minimization problem (9) is usually solved by using an alternating optimization scheme

$$u_i = \frac{\int_{\Omega} f \chi_i dx}{\int_{\Omega} \chi_i dx} \quad (10)$$

and

$$\begin{aligned} \frac{\partial \phi_j}{\partial t} = \delta(\phi_j) \left(\gamma \text{div} \left(\frac{\nabla \phi_j}{|\nabla \phi_j|} \right) - \sum_{i=1}^n Q_i \frac{\partial \chi_i}{\partial \phi_j} \right) \\ + \mu \left(\Delta \phi_j - \text{div} \left(\frac{\nabla \phi_j}{|\nabla \phi_j|} \right) \right) \end{aligned} \quad (11)$$

Theoretically, μ should be a large penalty parameter, but it was pointed out in [12] that the time step $\Delta t > 0$ and the parameter $\mu > 0$ must satisfy $\mu \Delta t < 0.25$ for stability. Therefore, there is a contradiction between the accuracy of the constraint and the choice of large time steps.

To improve the accuracy and stability, the authors in [14] introduce an ALM to solve the segmentation problem in (8). Define $D_j(\phi_j) = |\nabla \phi_j| - 1$, the augmented Lagrangian functional is

$$\begin{aligned} \max_{\bar{\lambda}_j} \min_{\phi_j} \left\{ \sum_{j=1}^m \gamma \int_{\Omega} \delta_{\varepsilon}(\phi_j) |\nabla \phi_j| dx + \sum_{i=1}^n \int_{\Omega} Q_i \chi_i dx \right. \\ \left. + \sum_{j=1}^m \int_{\Omega} \bar{\lambda}_j D_j dx + \sum_{j=1}^m \frac{\mu}{2} \int_{\Omega} D_j^2 dx \right\} \end{aligned} \quad (12)$$

where $\bar{\lambda}_j$ is called the Lagrange multiplier.

The minimization of (12) is solved by the following iterative scheme

$$\begin{aligned} \frac{\partial \phi_j}{\partial t} = & \gamma \delta_\varepsilon(\phi_j) \operatorname{div} \left(\frac{\nabla \phi_j}{|\nabla \phi_j|} \right) - \sum_{i=1}^n Q_i \frac{\partial \chi_i}{\partial \phi_j} \\ & + \operatorname{div} \left(\bar{\lambda}_j \frac{\nabla \phi_j}{|\nabla \phi_j|} \right) + \mu \left(\Delta \phi_j - \operatorname{div} \left(\frac{\nabla \phi_j}{|\nabla \phi_j|} \right) \right) \end{aligned} \quad (13)$$

and

$$\bar{\lambda}_j^{k+1} = \bar{\lambda}_j^k + \mu \left(|\nabla \phi_j^{k+1}| - 1 \right) \quad (14)$$

This method simplifies the treatment of constraint greatly, but it does not avoid the computation of curvature in evolution equation (13) as in (11).

III. THE PROPOSED METHOD

A. SALPM

The SALM in this section is inspired by the researches in [6, 7]. Different from the constraint $D_j = |\nabla \phi_j| - 1$ in (12), we introduce a new variable, say \bar{w}_j , to serve as the argument of the functional $D_j = \bar{w}_j - \nabla u_j$, under the constraint $\bar{w}_j = \nabla u_j$. This leads to the following constrained problem

$$\begin{aligned} \max_{\bar{\lambda}_j} \min_{\phi_j, \bar{w}_j} \left\{ \sum_{i=1}^n \int_{\Omega} Q_i \chi_i dx + \sum_{j=1}^m \gamma \int_{\Omega} \delta(\phi_j) |\bar{w}_j| dx \right. \\ \left. + \sum_{j=1}^m \int_{\Omega} \bar{\lambda}_j D_j dx + \frac{\mu}{2} \sum_{j=1}^m \int_{\Omega} D_j^2 dx \right\} \quad \text{s.t. } |\bar{w}_j| = 1 \end{aligned} \quad (15)$$

Note here that the SALM reduces the possibility of ill-conditioning by introducing the Lagrangian multiplier $\bar{\lambda}_j$ and variable \bar{w}_j at each step into the energy functional (15). Therefore, the convergence of this algorithm can be guaranteed without increasing μ to a very large value as the penalty method in (9).

Since (15) involves multiple variables, we also use the alternative minimization method to find the numerical solution to (15). A saddle point of the max-min problem (15) needs the following three equations

$$\begin{aligned} \gamma |\bar{w}_j^k| \frac{\partial \delta(\phi_j)}{\partial \phi_j} + \sum_{i=1}^n Q_i \frac{\partial \chi_i}{\partial \phi_j} + \operatorname{div}(\bar{\lambda}_j^k) \\ - \mu \left(\Delta \phi_j - \operatorname{div}(\bar{w}_j^k) \right) = 0 \end{aligned} \quad (16)$$

$$\gamma \frac{\bar{w}_j}{|\bar{w}_j|} \delta_\varepsilon(\phi_j^{k+1}) + \bar{\lambda}_j^k + \mu (\bar{w}_j - \nabla \phi_j^{k+1}) = 0 \quad \text{s.t. } |\bar{w}_j| = 1 \quad (17)$$

$$\bar{\lambda}_j^{k+1} = \bar{\lambda}_j^k + \mu (\bar{w}_j^{k+1} - \nabla \phi_j^{k+1}) \quad (18)$$

We use the semi-implicit difference scheme and

Gauss-Seidel iterative method to obtain a steady-state solution to the sub-problem (16).

Minimization with respect to \bar{w}_j^{k+1} can be performed by using the following shrinkage operator [7]

$$\bar{w}_j^{k+1} = \max \left(\left| \nabla \phi_j^{k+1} - \frac{\bar{\lambda}_j^k}{\mu} \right| - \frac{\gamma}{\mu} \delta_\varepsilon(\phi_j^{k+1}), 0 \right) \frac{\left(\nabla \phi_j^{k+1} - \frac{\bar{\lambda}_j^k}{\mu} \right)}{\left| \nabla \phi_j^{k+1} - \frac{\bar{\lambda}_j^k}{\mu} \right|}, 0 \frac{\bar{\mathbf{0}}}{|\bar{\mathbf{0}}|} = \bar{\mathbf{0}} \quad (19)$$

At last, \bar{w}^{k+1} is obtained via a simple projection technique as

$$\bar{w}_j^{k+1} = \frac{\bar{w}_j^{k+1}}{|\bar{w}_j^{k+1}|} \quad (20)$$

B. Algorithm Details

Now we present the iterative augmented Lagrangian projection method in Algorithm I.

Algorithm I (SALPM)

1. **Initialization:** $\phi_j^0, \bar{\lambda}_j^0, \bar{w}_j^0$ and set $k = 0$,
for $i = 1, 2, \dots, n, j = 1, 2, \dots, m$.
 2. **Repeat**
 3. Update each u_i^{k+1} by (10);
 4. Compute each ϕ_j^{k+1} by (16);
 5. Compute each \bar{w}_j^{k+1} by (19) and (20);
 6. Compute each $\bar{\lambda}_j^{k+1}$ by (18);
 7. $k = k + 1$;
 8. **Until** a stopping criterion $|E^{k+1} - E^k|/E^k \leq \eta$ is satisfied, where η is a small positive value.
-

IV. EXPERIMENTAL RESULTS

This section shows numerical results of our SALPM for both synthetic and real images. All the experiments are performed by using MATLAB v2010b on a Windows XP platform with an Intel Core 2 Duo CPU at 2.80 GHz and 2GB memory. To set up a relatively neutral criterion for comparison, we use the same initial contour for all the methods in each experiment. Moreover, some parameters are fixed for generality as follows: $\varepsilon = 2, \Delta t = 0.02$. γ is required to be tuned for each example, and is usually formatted by $\gamma = \alpha \times 255^2, \alpha \in (0, 1)$.

A. Comparison and Analysis of Two-phase Experiments

We first compare our proposed algorithm to re-initialization method in [10], Li et al.'s method in [12] and ALM in [14] designed to preserve the SDF in the LSM. The test image is presented in Fig. 1(a). For the re-initialization method, the initial LSF is an SDF. The initial LSF for the other three approaches is a piecewise

constant function. Numerically, we can check that the four methods give the same solution as shown in Fig. 1(b). Figs. 1(c), 1(e), 1(g), and 1(i) show the evolution of the level set function for the four different methods. In Figs.

1(d), 1(f), 1(h), and 1(j), we plot the corresponding mean deviation of $|\nabla\phi^k| - 1$, which measures the distance between the computed LSF at the k th iteration.

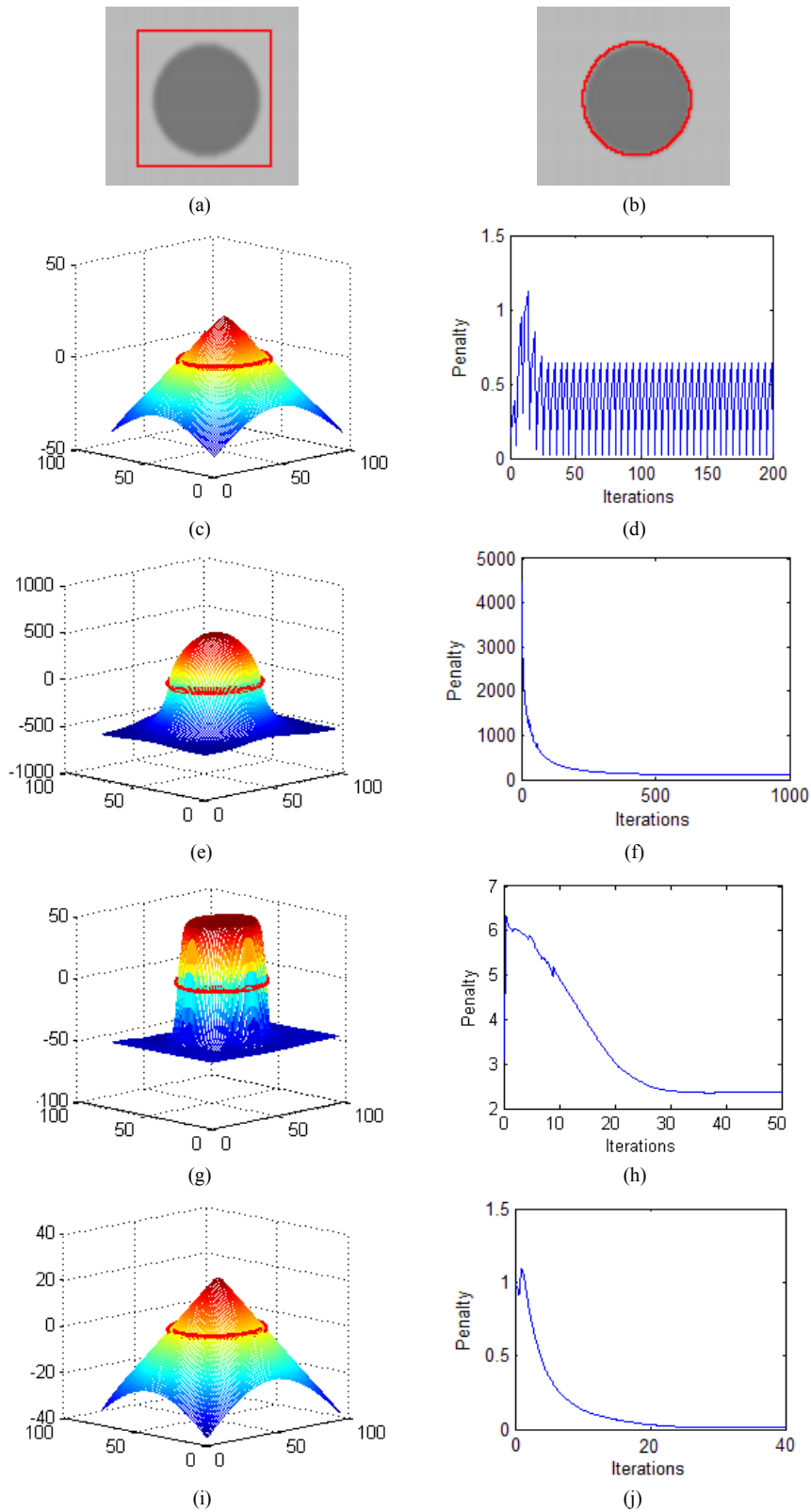


Figure 1. Segmentation of circle image with two phases. (a) Test image of size 100x100; (b) Same segmentation result using re-initialization method, Li et al.'s method, ALM and SALPM, respectively; (c)-(d) Results with re-initialization for $\gamma = 0.01 \times 255^2$; (e)-(f) Results with Li et al.'s method for $\gamma = 0.01 \times 255^2$; (g)-(h) Results with ALM for $\gamma = 0.1 \times 255^2$; (i)-(j) Results with SALPM for $\gamma = 0.01 \times 255^2$.

Although the final LSF provides the desired results in Fig. 1(c), the periodic re-initialization process produces a non-smooth minimization in Fig. 1(d). Besides, we do not know in general when to re-initialize the LSF as an SDF. In this experiment, we apply the re-initialization for every 5 iteration. We then consider the penalty method in [12]. Fig. 1(e) shows their method does not constrain exactly the LSF to be an SDF. Moreover, their approach slows down the minimization process as the

number of iterations to reach the convergence state increases considerably as shown in Fig. 1(f). We observe from Fig. 1(g) that the ALM in [14] converges faster than Li et al.'s method, but the LSF differs from an SDF. Our algorithm is presented in Figs. 1(i) and 1(j). Our formulation constrains the LSF to be an SDF due to projections, and the proposed SALPM is fast because it avoids the calculation of the curvature term.

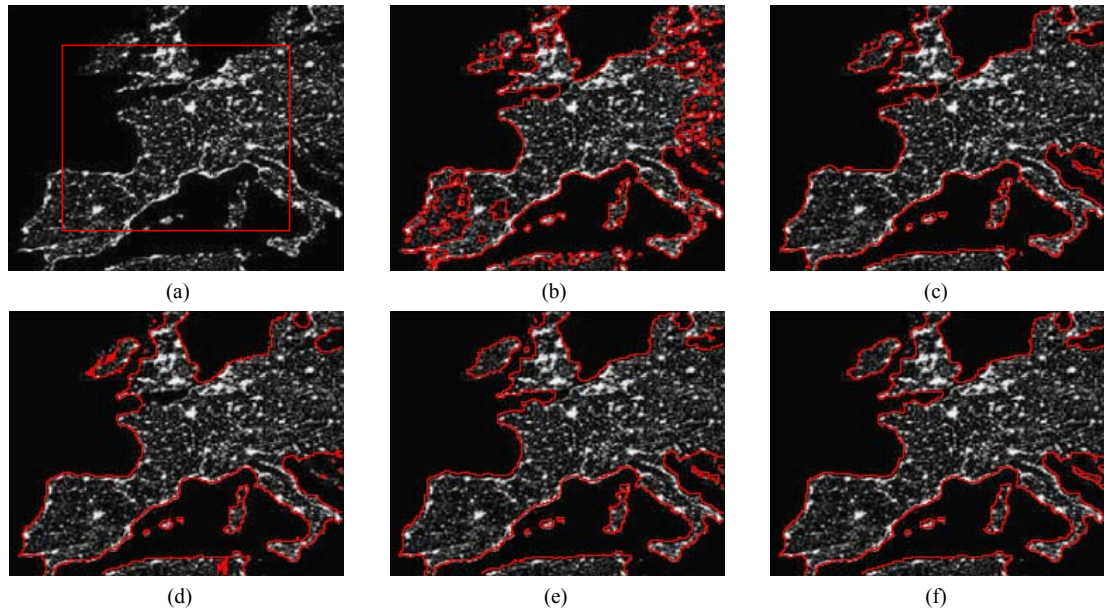


Figure 2. Segmentation of Europe night-lights image with two phases. (a) Test image of size 238x188; (b) Result with no re-initialization for $\gamma = 0.05 \times 255^2$; (c) Result with re-initialization for $\gamma = 0.05 \times 255^2$; (d) Result with Li et al.'s method for $\gamma = 0.1 \times 255^2$; (e) Result with ALM for $\gamma = 0.05 \times 255^2$; (f) Result with SALPM for $\gamma = 0.01 \times 255^2$.

Next, we show the segmentation results on a natural Europe night-lights image in Fig. 2(a). We can see from Figs. 2(b) and 2(c) that the segmentation results visually have different topologies for the two-phase Chan-Vese model with no or with re-initialization process using the same parameters, which demonstrates that whether or not the re-initialization is done affects segmentation

accuracy. Then the segmentation results by Li et al.'s method, ALM and our SALPM are given in Fig. 2(d)-(f). From the segmentation results, we see that all the three methods work for this image and get the satisfactory results. However, when better and detailed segmentation results are needed, our proposed method indeed performs better in Fig. 2(f).

TABLE I
COMPARISON OF ITERATIONS AND COMPUTATION TIME USING DIFFERENT SEGMENTATION METHODS

Methods	Iterations				CPU time (s)			
	Fig. 1	Fig. 2	Fig. 3	Fig. 5	Fig. 1	Fig. 2	Fig. 3	Fig. 5
Re-initialization method [10]	200	217	-	-	9.34	11.23	-	-
Li et al.'s method [12]	1000	318	235	216	8.51	8.37	17.49	11.94
ALM [14]	50	47	67	59	3.68	1.92	5.71	3.03
SALPM	33	34	45	41	1.85	1.09	3.09	1.46

See Table I for the corresponding iterations and computation time for segmentation of this example. For the re-initialization method, a lot of time is spent on re-initialization. Li et al.'s method is faster than the re-initialization method, although it requires a considerable number of iterations. We can see that the ALM and our

method are much faster than both of the re-initialization method and Li et al.'s method. Moreover, our method is much faster than the ALM due to simple computation of Laplacian, generalized soft thresholding formula and projection.

B. Comparison and Analysis of multiphase Experiments

To provide some more insights, we compare our SALPM with the Li et al.'s method and ALM on multiphase image segmentation. Fig. 3(a) is a synthetic image with three regions. Fig. 3(b) is the degraded image with Gaussian noise. We observe from Figs. 3(c)-3(e) that

three algorithms work for this noisy image and get the desirable results, but our method gives better segmentation results than the other two methods. In Fig. 4, we present quantitative comparisons among the three methods by giving the plots of the error ratio (denoted as ER [21]) vs. the iteration number. Here, the results are consistent with the conclusion in Fig. 3.

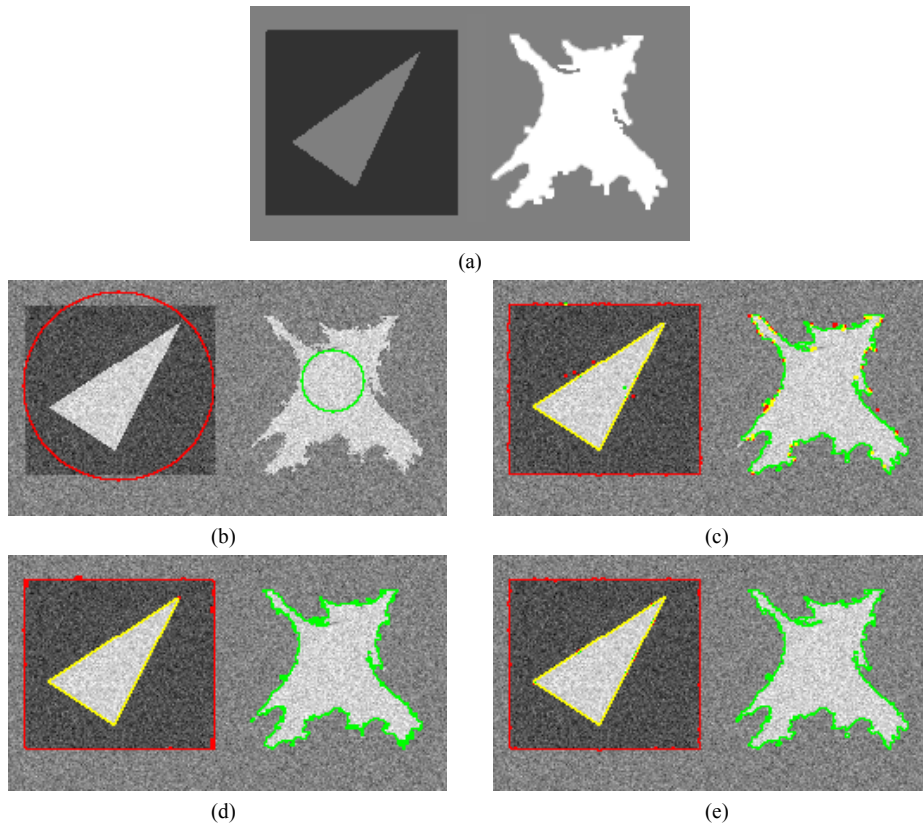


Figure 3. Segmentation of synthetic image with three phases. (a) Original synthetic image of size 256×128 ; (b) Degraded image and the same initial contour for all the methods; (c) Result with Li et al.'s method for $\gamma = 0.1 \times 255^2$; (d) Result with ALM for $\gamma = 0.05 \times 255^2$; (e) Result with SALPM for $\gamma = 0.01 \times 255^2$.

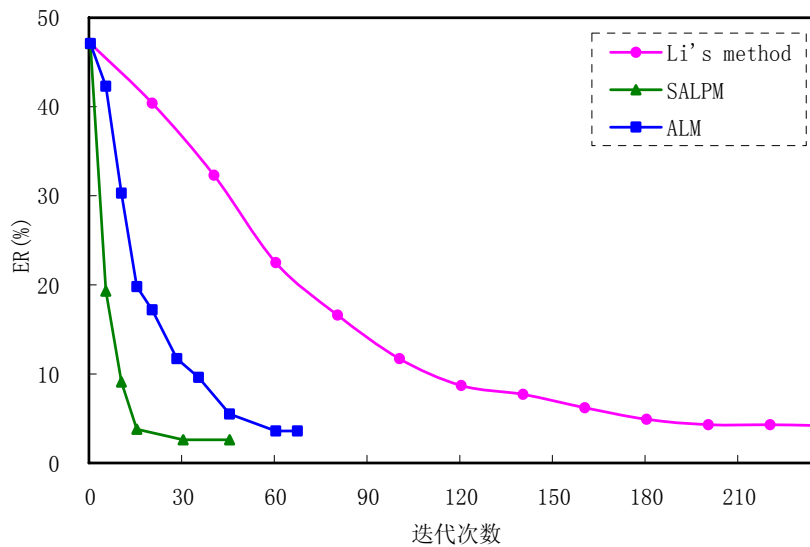


Figure 4. Evolution of error ratio for segmentation of the synthetic image using different methods.

In Fig. 5, we present the experimental results for four-phase natural image segmentation of the Li et al.'s method, ALM and SALPM. Again, we observe from Figs. 4(b)-(d) that our algorithm exhibits a better

performance than the other two in the aspect of segmentation accuracy. Meanwhile, we conclude from Table I that the SALPM converges faster and consumes less time than any of the other methods.

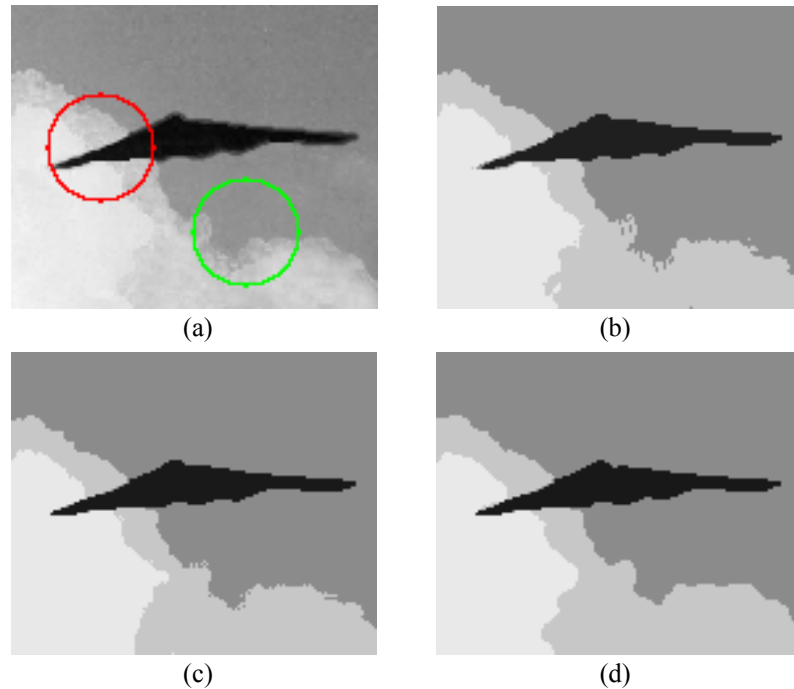


Figure 5. Segmentation of real image with four phases. (a) Test image of size 139×115 ; (b) Result with Li et al.'s method for $\gamma = 0.1 \times 255^2$; (c) Result with ALM for $\gamma = 0.05 \times 255^2$; (d) Result with SALPM for $\gamma = 0.01 \times 255^2$.

V. CONCLUSIONS

In this paper, we have introduced a new variational level set formulation that completely eliminates the need of the re-initialization and overcomes the speed limitation. By introducing some auxiliary variables, we design its fast split augmented Lagrangian projection method, which does not involve difference of curvatures, and can preserve SDFs automatically via a simple projection. In addition, even if the initial LSF is not an SDF, it can be corrected automatically.

The idea of this paper can be easily extended to other models under the variational level set framework, such as motion segmentation, 3D reconstruction, and geometric surface processing etc.

ACKNOWLEDGMENT

This work was supported by National Natural Science Funds of China (No. 61170106).

REFERENCES

- [1] S. Osher, and J. A. Sethian, "Fronts propagating with curvature-dependent speed: Algorithms based on Hamilton-Jacobi formulation," *Journal of Computational Physics*, vol. 79, no. 1, pp. 12-49, 1988.
- [2] T. Andersson, G. L  th  n, R. Lenz, and M. Borga, "Modified gradient search for level set based image segmentation," *IEEE Transactions on Image Processing*, vol. 22, no. 2, pp. 621-630, 2013.
- [3] H. Zhang, Z. Duan, Z. Zhu, and Y. Wang, "Fast moving object segmentation based on active contours," *Journal of Computers*, vol. 7, no. 4, pp. 863-869, 2012.
- [4] J. Lie, M. Lysaker, and X.-C. Tai, "A binary level set model and some applications to Mumford-Shah image segmentation," *IEEE Transactions on Image Processing*, vol. 15, no. 5, pp. 1171-1181, 2006.
- [5] T. F. Chan, S. Esedoglu, and M. Nikolova, "Algorithms for finding global minimizers of denoising and segmentation models," *SIAM Journal on Applied Mathematics*, vol. 66, no. 5, pp. 1632-1648, 2006.
- [6] X. Bresson, S. Esedoglu, P. Vandergheynst, J.-P. Thiran, and S. Osher, "Fast global minimization of the active contour/snake model," *Journal of Mathematical Imaging and Vision*, vol. 28, no. 2, pp. 151-167, 2007.
- [7] T. Goldstein, X. Bresson, and S. Osher, "Geometric applications of the Split Bregman method: Segmentation and surface reconstruction," *Journal of Scientific Computing*, vol. 45, no. 1, pp. 272-293, 2010.
- [8] C. Liu, Y. Zheng, Z. Pan, J. Duan, and G. Wang, "SAR image segmentation based on fuzzy region competition method and Gamma model," *Journal of Software*, vol. 8, no. 1, pp. 228-235, 2013.
- [9] V. Estellers, D. Zosso, R. Lai, S. Osher, J.-P. Thiran, and Xavier Bresson, "Efficient algorithm for level set method preserving distance function," *IEEE Transactions on Image Processing*, vol. 21, no. 12, pp. 4722-4734, 2012.
- [10] M. Sussman, P. Smereka, and S. Osher, "A level set approach for computing solutions to incompressible two-phase flow," *Journal of Computational Physics*, vol. 114, pp. 146-159, 1994.

- [11] J. Gomes, and O. Faugeras, "Reconciling distance functions and level sets," *J. Vis. Commun. Image Represent.*, vol. 11, no. 2, pp. 209-223, 2000.
- [12] C. Li, C. Xu, C. Gui, and M. D. Fox, "Level set evolution without re-initialization: A new variational formulation," *Proceedings of IEEE Computer Society Conference on Computer Vision and Pattern Recognition (CVPR)*, vol. 1, pp. 430-436, 2005.
- [13] C. Li, C. Xu, C. Gui, and M. D. Fox, "Distance regularized level set evolution and its application to image segmentation," *IEEE Transactions on Image Processing*, vol. 19, no. 12, pp. 3243-3254, 2010.
- [14] C. Liu, F. Dong, S. Zhu, D. Kong, and K. Liu, "New variational formulations for level set evolution without reinitialization with applications to image segmentation," *Journal of Mathematical Imaging and Vision*, vol. 41, pp. 194-209, 2011.
- [15] K. Zhang, L. Zhang, H. Song, and D. Zhang, "Reinitialization-free level set evolution via reaction diffusion," *IEEE Transactions on Image Processing*, vol. 22, no. 1, pp. 258-271, 2013.
- [16] R. Courant, K. Friedrichs, and H. Lewy, "On the partial difference equations of mathematical physics," *IBM J.*, vol. 11, no. 2, pp. 215-234, 1967.
- [17] T. F. Chan, and L. A. Vese, "Active contours without edges," *IEEE Transactions on Image Processing*, vol. 10, no. 2, pp. 266-277, 2001.
- [18] L. A. Vese, and T. F. Chan, "A multiphase level set framework for image segmentation using the Mumford and Shah model," *International Journal of Computer Vision*, vol. 50, no. 3, pp. 271-293, 2002.
- [19] H.-K. Zhao, T. F. Chan, B. Merriman, and S. Osher, "A variational level set approach to multiphase motion," *Journal of Computational Physics*, vol. 127, no. 1, pp. 179-195, 1996.
- [20] Q. Wang, Z. Pan, and W. Wei, "Split-Bregman method and dual method for multiphase image segmentation," *Journal of Computer-Aided Design & Computer Graphics*, vol. 22, no. 9, pp. 1561-1569, 2010.
- [21] S. Han, W. Tao, and X. Wu, "Texture segmentation using independent-scale component-wise Riemannian-covariance Gaussian mixture model in KL measure based multi-scale nonlinear structure tensor space," *Pattern Recognition*, vol. 44, no. 3, pp. 503-518, 2011.

Cunliang Liu was born in 1977. He received Ph.D. degree in the college of information science & engineering, Shandong University of Science & Technology, Qingdao, China, in 2012. He is currently a lecturer in the College of Information Engineering at Qingdao University. His research interests include image segmentation, the variational methods and PDEs in image processing.

Zhenkuan Pan was born in 1966. He received his Ph.D. degree in the engineering mechanics from Shanghai Jiao Tong University, China in 1992. Currently he is a professor of the College of Information Engineering at Qingdao University. His research interests include dynamics and control of multibody systems, computer simulation and variational image processing. He has published numerous papers and conference papers in the area of image processing and object recognition.

Jinming Duan was born in 1989. Currently he is a postgraduate student of the College of Information Engineering at Qingdao University. His research interests include variational image processing, and three-dimensional reconstruction.